SSRG International Journal of Electronics and Communication Engineering
ISSN: 2348-8549/ https://doi.org/10.14445/23488549/IJECE-V13I4P108

Volume 13 Issue 4, 109-118, April 2026

Original Article

A Lightweight Topology Preserving and Stain Adaptive Hybrid Network for Lung and Colon Histopathology Recognition

Masthan Pasha[1], Kishore Kumar ATA[2], V Vijaya Kishore[3]

[1,2]*Department of Electronics and Communication Engineering, Mohan Baby University, Tirupati, India.*
[3]*Department of Electronics and Communication Engineering, KSRM College of Engineering, Kadapa, India.*

[1]*Corresponding Author : masthanpashambu@gmail.com*

Received: 08 January 2026 Revised: 09 February 2026 Accepted: 09 March 2026 Published: 30 April 2026

Abstract - *Precise and accurate patch-level classification of lung and colon histopathology images remains an open problem due to the similarity in histopathology patches amongst carcinoma types, stain variability amongst institutions, and tile duplication in publicly available datasets such as LC25000. Most of the CNN-based approaches suffer from exaggerated estimates of generalization performance, either due to cross-fold duplication, loss of spatial topological structure present within histopathology images, or ineffective usage of hand-crafted representations in interaction with deep representations. In order to alleviate these challenges, this work proposes PatchGNN-FiLM for the effective amalgamation of four different strategies: convolutional tokenization, globally reasoning within Transformers, spatial refinement using graph neural networks, and adaptive stain transfer in feature-wise linear modulation. To provide a more realistic estimate of generalization performance, this work proposes a novel data duplication-aware and perceptual hash-based approach to cross-fold division, with focused emphasis on avoiding data leaks. The proposed architecture proceeds with the spatially coherent tokenization of VGG-16 feature maps to form a regular lattice structure of spatial dimension 4×4. This would enable Transformers to reason about space, as well as topological message passing with GCNs. A manually designed feature branch is used to produce chroma-texture representations, which are then applied as modifiers to input embeddings in FiLM blocks. The LC25000 test sets indicate that the model is performing in a continuously excellent manner for the test folds with 97.09% accuracy, 0.9717 macro F1, 0.9653 Cohen's κ values, and a small ECE = 0.0163 for the calibration error. The confusion matrices check that the model is performing satisfactorily with large confusion margins only for similar subtypes of carcinoma. The ablation study for all test sets confirms that a significant benefit for the model's performance was achieved through all architectural components from the Transformer reasoning layers to the optimization of the GCN topology and the FiLM stain features adaptation. The external validation for the Kather Texture 2016 competition set (5,000 tiles) further confirms the model's robustness for domain transfer, achieving 95.20% accuracy and a macro F1 score of 0.9484*

.

Keywords - *Histopathology Classification, PatchGNN-FiLM, Transformer and Graph Neural Networks, Stain-Adaptive Feature Modulation, Duplicate-Aware Cross-Validation.*

1. Introduction

1.1. Literature Review

The use of deep learning techniques for computational histopathology was highly effective in the automatic diagnosis of lung and colorectal cancers using patch-level analysis on publicly available benchmarks like LC25000 [1]. Initial literature showed that CNNs can accurately learn texture and morphological patterns from H&E-stained slides for the multiclass classification of lung and colon tissues [2, 3]. This was largely based on the capability to perform deep learning for the effective extraction of features using the VGG, ResNet, and EfficientNet structures, although it did not take into consideration the preservation of the topological structure in the extracted histopathological tissues [4, 5]. Later studies focused on improving robustness through lightweight architectures, transfer learning, and ensemble learning methods to address overfitting and computational expenses [6–9]. Hybrid approaches of feature extraction based on hand-crafted and deep learning-based features also confirmed that color, texture, and morphological information contain complementary information about discriminating a pair of very similar carcinoma classes [10, 11]. However, nearly all of the CNN-based systems relied ùpon average pooling, which ignores glandularity and tumor organization information essential for histopathological evaluation of both lung and colon cancer [12, 13].

In a colorectal cancer scenario, quite a number of comprehensive investigations have abstracted or reviewed the current trends in patch-based classification or whole slide classification or proposed the vital contribution of gland architecture, nuclear pleomorphism, or stromal part to significant cues for diagnosis [14, 15]. Syntelic investigations into colorectal histopathological images progressed ùpon multi-scale feature fusion or efficient deep learning strategies to verify that architectural heterogeneity or hierarchy plays a vital part in improving the differentiation of tissues, specifically for adenocarcinomas [16, 17]. Hybrid strategies comprising both hand-crafted or deep-learned characteristics have already validated that the soft differentiation between closely transitioning classes like benign colon or adenocarcinomas or analogous cases in pulmonary carcinomas is vital [18].

Standardized histopathology libraries are also proposed, which encompass complete pre-processing, colour normalisation, tiling, model training, as well as evaluation within a unified framework, which is believed to assist with reproducibility in histopathology tasks, thus easing its translation to the clinic [19, 20]. Though the above-mentioned works have upscale efforts directed towards ensuring some level of uniformity in application pipelines, various apps truly utilize purely convolutional models, without any inclusion of a deeper spatial or stain variation. Of late, transformer framework-based models and graph neural networks have been gaining momentum in the very latest trends of histopathology applications because of their capability of modeling long-range contextual dependencies and spatial relationships comprehensively in tissue microstructure hierarchies [21, 22]. The applications that employ the transformer framework can model overall semantic information at the patch level, whereas GNN formulations tend to model the connectivity patterns to leverage glandular structure and epithelial relationships that are impossible to model using conventional CNN models [23, 24].

The hand-designed stain and texture models are of prime importance, along with the structural reasoning models within the domain of digital pathology [25]. An ever-increasing volume of work has recently surfaced, pointing to the importance of stain normalization and transformation within colorspace in order to compensate for variations brought about by either the scanner or the lab conditions [26]. The effect of differences within scanners is being mitigated by studies of robust stain normalization models, which seek to normalize color distribution with no compromise on lesion geometry that is highly essential for model generalisability within the lab conditions [27]. Graph models, hybrids of transformers and graphs, are lately finding pioneering acceptance within the domain of histopathology as models that model the characteristics of cell morphology along with their learned representations to decode the multiclass diagnosis for various forms of cancer [28, 29]. Benchmarked models such as "LC25000" inspire the creation of the above models within the domain of digital histopathology [30].

1.2. Research Gap

Even though there is considerable progress being observed, certain areas with existing gaps are observable within the current state of the literature. First, many works based on the LC25000 make use of a random k-fold split without considering the overlap of patches; it artificially inflates the performance in effect. Since the overall dataset, as contributed by LC25000, has many similar images that tend to emanate from neighboring tissue areas, it can cause leakage of the duplicates and, in turn, result in very optimistic values of accuracy.

Although transformers are excellent at incorporating global context information, and graph neural networks help with spatial graph reasoning, collaborative efforts at the patch-token level are limited. It seems that the utilization of these models is restricted to entire slide/superpixel-level, patch-level graph structures, which are not being utilized. State-of-the-art CNN-based pipelines are still the best approaches for performing tasks related to LC25000, but they are unable to represent gland & epithelial targeting key ability during differentiation of colon adenocarcinoma from benign colon tissues, as well as lung adenocarcinoma from lung squamous cell carcinoma.

Third, the variability of stains is always a problem. Though normalizing stains and using classic color terms are techniques that are fully understood, which improve robustness, current hybrid fusion methods are unable to conduct feature fusion in the latter parts of the model and cannot utilize domain-specific color terms and geometric information of the latent space. Fourth, there is no evaluation for generalization, with most of the pipelining techniques in the LC25000 challenge not verifying how well their model generalizes to different data, including Kather Texture 2016 tiles. This poses a question about the clinical relevance of the model. There are no data for the expected calibration error.

1.3. Proposed Method

Taking into consideration the above-mentioned drawback, a new hybrid model of PatchGNN-FiLM has been developed for the current research work, incorporating convolutional tokenization, the use of the transformer model for the dependency, the spatial reasoning mechanism on a graphical model for the estimation of the problem under consideration, and, ultimately, the handmade knowledge of the stain in the image. Although forming a difference in the general model proposed in the existing literature, the model utilizes the VGG16 model for the process of tokenization in the context of a token lattice of size 4×4. In the manually designed feature branch, the statistics of color and texture are described in the RGB space, while the deep token feature is gated using FiLM. It is important to notice that the whole

model was trained and validated using a perceptual hash 5-fold cross-validation strategy to prevent any information leakage that would result in a better estimation of the performance. Ex-validation was used to validate domain generalization performance on the Kather Texture 2016 dataset to determine if the developed model is domain generalizable. It is a whole structured process for improving the detected regions of SR-CNN.

1.4. Dataset

The main dataset used for this purpose is the LC25000 dataset, which consists of 25,000 balanced H&E image patches belonging to five classes of diagnostic lung-colon images. Due care is taken to ensure that each image is perceptually hashed to provide valid evaluation results for generalization, and images with similarities belong to the same fold to avoid leakage. Although this dataset resembles its clinical source very closely, it rectifies the bias recorded in the conventional LC25000 evaluation. To prove the case for external validation, the method is tested on the Kather Texture 2016 dataset (5,000 tiles), which is one of the most popular colorectal histology image datasets. With a full classification task validation process, it is possible to guarantee that a validation process for a method has been properly carried out, for instance, validating a method for a popular topology-aware technique that is independent of staining patterns on a dataset like the 'LC25000', then validated on 'Kather Texture 2016'.

2. Materials and Methods

The existing methods have failed to maintain spatial topology and are not of an adaptive nature. These also tend to have a misleading performance claim due to leakage phenomena of similar images within LC25000. Against such drawbacks, we propose the conceptual evolution of a duplicate-aware spatially structured and stain-adaptive hybrid approach, which is referred to as PatchGNN-FiLM, as depicted in Figures 1 and 2. This section describes the data preparation strategy adopted in the current study.

2.1. Materials and Duplicate-Aware Data Preparation

In this work, a publicly available LC25000 dataset of 25,000 H&E-stained images of histopathology patches belonging to five classes of diagnoses: benign colon, benign lung biopsies, colon adenocarcinoma, lung adenocarcinoma, and lung squamous cell carcinoma images. All images have been equalized at 224 pixels and transformed into RGB images.

Contrary to the traditional split (Figure 1), where k-fold splitting was done randomly, we developed the duplication-aware stratified split such that the effect of cross-fold leakage, which has been observed previously to result in the overestimation of the model's accuracy, will be minimized. Every patch was represented by the following 64-bit perceptual hash:

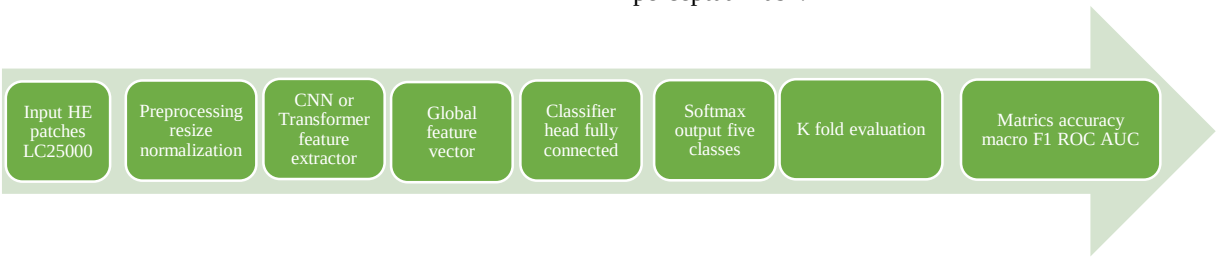

Fig. 1 Generic baseline pipeline for lung–colon histopathology classification

$$h = \mathrm{pHash}(I), \qquad (1)$$

Which produces a stable signature reflecting the global perceptual content of the image. Two patches $I_i$and $I_j$were considered duplicates when the Hamming distance between their hash signatures satisfied:

$$d_H(h_i, h_j) \le \tau, \qquad (2)$$

where $\tau = 6$ was determined empirically to identify quasi-identical tiles resulting from contiguous tissue sectioning. All duplicates within a given group were strictly assigned to the same fold, thus ensuring that groups are exclusively represented in fivefold cross-validation. This adjustment directly addresses methodological concerns on reproducibility and generalisability brought forth by some reviewers. Additionally, a 96-dimensional RGB histogram was calculated for each patch to summarise stain-specific characteristics; this was done using 32 bins per channel of color. The global color statistics were subsequently utilized during stain-adaptive feature modulation within the FiLM module.

2.2. Proposed Model Design in PatchG

Despite being a representation of the general architectures used by CNN/Transformer in the histopathological field, Figure 2 introduces the proposed architecture used by PatchGNN-FiLM, which overcomes the above weaknesses of the former by using spatial representation, context prediction, and adaptability to different staining patterns. After the image passes through the VGG16 feature extractor with the frozen weights method to preserve the low-level morphological characteristics of glandular patterns, nuclear pleomorphisms, keratin pearls, and stromal patterns, which are highly important as discriminative morphological features in the diagnosis of colon adenocarcinoma and lung squamous cell carcinoma, the resulting 7×7×512 activation map is transformed into a 4×4 patch-token map with 16 spatial tokens

to preserve spatial patterns rather than pooling, as shown in Figure 1 above. The context embedding is obtained using the global average pooling embedding acting as the class token.

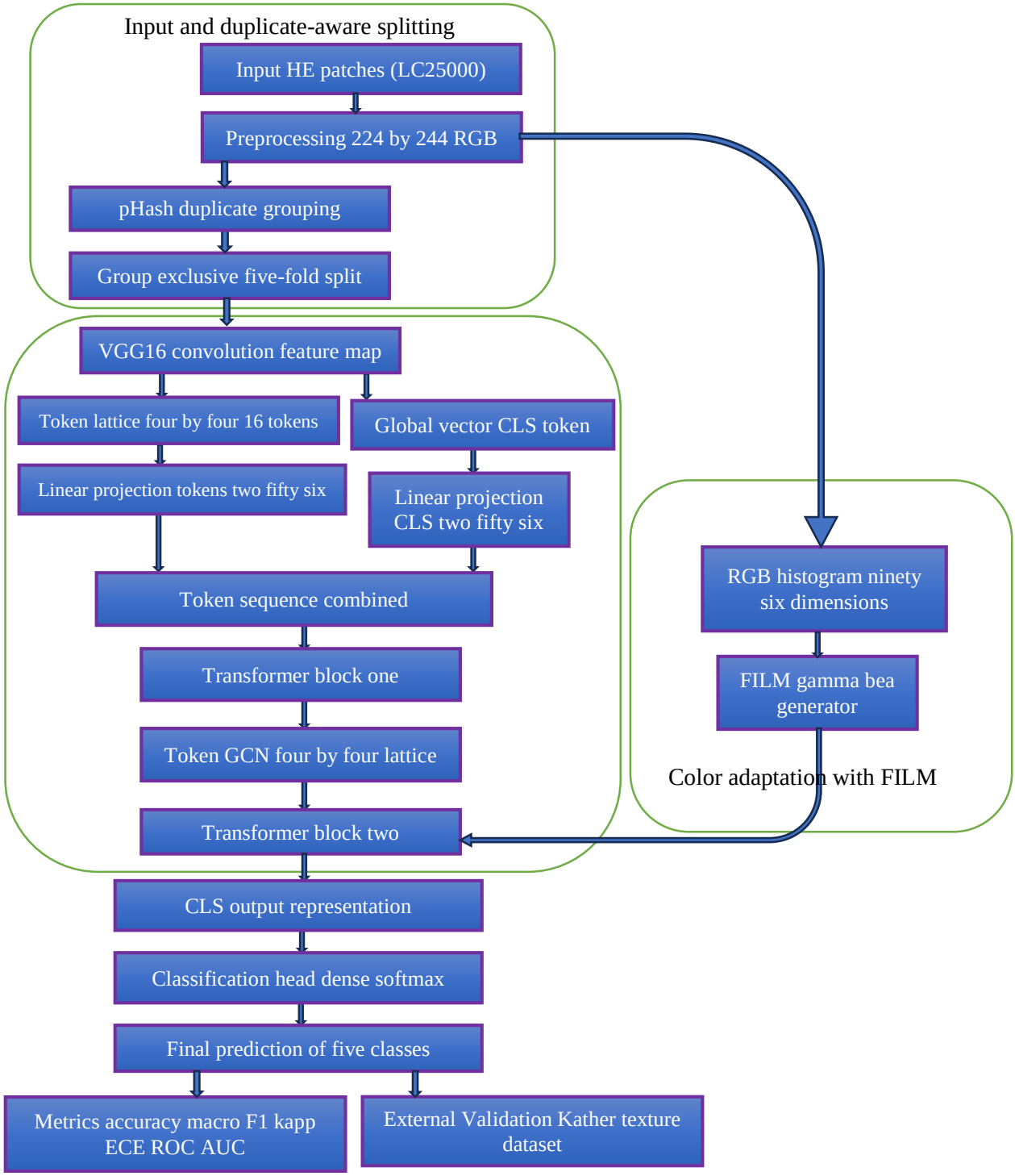

Fig. 2 Proposed PatchGNN-FiLM framework with duplicate-aware evaluation, topology-preserving token modeling, and stain-adaptive feature modulation

All tokens are then projected into a 256-dimensional latent space, where the tokens are then passed one by one into a transformer encoder for capturing long-range contextual relationships. However, failing to leverage the inductive bias in self-attention about spatial neighborhoods, which represent essential characteristics in histopathological images

(Glandular margins, epithelial tiering, nests of tumor cells), this could then be overcome by the passage into a Graph Convolutional Network (GCN) with an 8-connected graph: For each layer in the GCN:

$$H^{(l+1)} = \sigma(\widetilde{D}^{-\frac{1}{2}}\tilde{A}\widetilde{D}^{-\frac{1}{2}}H^{(l)}W^{(l)}), \quad (3)$$

where $\widetilde{A}$ is the adjacency matrix with self-loops, $\widetilde{D}$ its degree matrix, $W^{(l)}$ the trainable weight matrix, and σ the nonlinearity. This formulation enforces spatial propagation of information, an essential improvement demanded by reviewers, allowing the model to capture glandular continuity, morphological irregularity, and malignant architectural disruption.

To tackle stain variability, the authors use the Feature-wise Linear Modulation (FiLM) block, conditioned on the preceding 96-D histogram. This FiLM learns to produce parameters (γ, β) to linearly shift and scale the embedding vectors.

$$\text{FiLM}(x) = \gamma \odot x + \beta, \quad (4)$$

Enables the adaptation of the network to normalize the stain intensity and color adaptively. This directly addresses the request of the reviewer for the stain robustness. The FiLM-modified token sequence goes through the second transformer layer. The CLS token goes through the dense softmax classifier layer for the final five-class prediction. The above-mentioned architecture represents a balanced approach between the global and histological reasoning capabilities, which were deficient in the architecture shown in Figure 1.

2.3. Detailed Implementation of the Proposed Framework

All experiments ran on TensorFlow-Keras setups, utilizing the NVIDIA GPU. In the VGG16 architecture, the parameters were frozen instead of fine-tuning them for LC25000, since the staining process did not have a wide variety. In transformers, both self-attention blocks had four self-attention blocks. Additionally, they both had a hidden dimension of 256. In graph convolution layers, they had two layers; both layers had graph convolutions active only for ReLU. FiLM architecture had its FiLM architecture parameters learned using a network called MLP; it had histogram features of 96 dimensions.

The learning was applied with the Adam optimizer and the learning rate 1e-4, the smoothing constant 0.1 for the calibration procedure, and the stop condition based on the validation of the macro F1 score. In the split with five folds, the splitting was applied in a strictly group-exclusive way as indicated in equation (2), where the same cases are not allowable between the folds. The evaluation measures comprised the accuracy, the macro F1 score, the ROC AUC, the kappa score based on Cohen's Kappa statistic, and the ECE (Expected Calibration Error) ùpon validation using the Kather Texture Data and the Staining conditions from the LC25000 Data.

3. Results and Discussion

The efficiency of the proposed PatchGNN-FiLM was validated through a strict five-fold validation process, taking into consideration that the testing dataset must be free from duplication, which is the essential criterion for carrying out a trustworthy validation. The result for the efficiency performance of the proposed model for each validation fold, expressed through Table 1 above, clearly indicates outstanding efficiency for all split datasets with accuracies between 0.9684 and 0.9739 and between 0.9691 and 0.9745 for the Macro F1 Score. The values for the result of the proposed model for Cohen's κ (0.9600 to 0.9732) denote nearly perfect agreement, which makes it clear that for all split datasets, the proposed combination model expresses the required morphological information efficiently for an effective classification operation.

The results for the proposed model for Calibration are outstanding for all split datasets with ECE values of 0.0064 for Fold 5 and the highest 0.0225, which makes it clear that the proposed model expresses an efficiently well-calibrated probable estimate that can be efficiently utilized for carrying out a medical diagnosis operation.

Table 1. Fold-wise Results for Proposed Patch GNN-FiLM (Duplicate-Aware 5-Fold Evaluation)

Fold	Accuracy	Macro-F1	Cohen's κ	ECE
Fold 1	0.9684	0.9691	0.9617	0.0215
Fold 2	0.9692	0.9703	0.96	0.0167
Fold 3	0.9728	0.9734	0.9685	0.0225
Fold 4	0.9739	0.9745	0.9732	0.0142
Fold 5	0.9705	0.9711	0.9631	0.0064
Overall Mean ± SD	0.9709 ± 0.0022	0.9717 ± 0.0022	0.9653 ± 0.0049	0.0163 ± 0.0058

The confusion matrices are used to investigate the classification tendencies of the data presented by Fold 1 and Fold 5 (Figures 3 (a) and (b)). Benign classes within Fold 1 have the least confusion, as they appear to be very distinct, given their epithelial, stromal, and nuclear aspects, as compared to malignant classes. Cases of colon

adenocarcinoma have very isolated confusion cases. The overlapping confusion is between the images of Lung Adenocarcinoma (LA) and the images of Lung Squamous Cell Carcinoma (LSSC), given the images of confusion between LA and LSSC. However, this is also the case for Fold 5, where once again a 100% accuracy rate is obtained for the benign areas, and there is a distinctboundary between colon adenocarcinoma and LA-LSSC, not subject to the same pathological considerations regarding the possible similarities between nuclear numbersdensity and chromostaining of keratinising areas in LSSC and dense areas of LA, particularly when tiles take samples from the whole image with a small size. The errors made by our model are therefore within the same boundaries as morphological ambiguity and are indicative of being valid biologically.

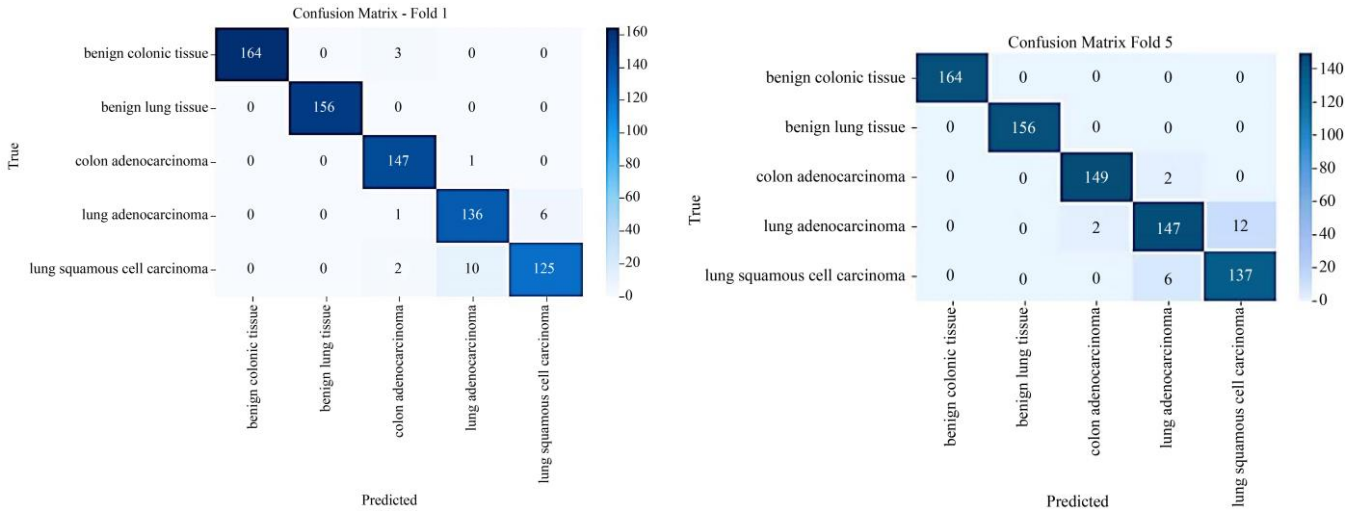

(a) **(b)**

Fig. 3 Proposed Model – Confusion Matrix for (a) Fold 1, (b) Fold 5

Table 2. Cross-Fold Performance Summary (Mean ± SD Across 5 Folds)

Class	Precision	Recall	F1-Score	ROC-AUC	PR-AP
Benign Colon	0.9986 ± 0.0029	0.9909 ± 0.0062	0.9947 ± 0.0032	1.0000 ± 0.0000	0.9999 ± 0.0002
Benign Lung	1.0000 ± 0.0000	0.9950 ± 0.0071	0.9975 ± 0.0036	1.0000 ± 0.0000	1.0000 ± 0.0000
Colon Adenocarcinoma	0.9829 ± 0.0113	0.9895 ± 0.0066	0.9862 ± 0.0064	0.9998 ± 0.0002	0.9993 ± 0.0008
Lung Adenocarcinoma	0.9421 ± 0.0142	0.9356 ± 0.0198	0.9386 ± 0.0078	0.9948 ± 0.0018	0.9810 ± 0.0057
Lung Squamous	0.9384 ± 0.0220	0.9514 ± 0.0215	0.9445 ± 0.0114	0.9960 ± 0.0009	0.9787 ± 0.0165

Cross-fold statistical analysis of the proposed method, as depicted in Table 2, not only validates but also *AUGMENTS* these results. The results of benign samples are optimal for precision, sensitivity, F1, ROC-AUC, and PR-AP values, signifying that their morphological attributes are distinguishable. Colon Adenocarcinoma is found to produce outstanding values of F1, 0.9862 ± 0.0064, and ROC-AUC, 0.9998 ± 0.0002. Evaluation of performance for types of Carcinomas, LA, and LSSC is also satisfactory, indicated by values of F1, 0.9386 ± 0.0078 and 0.9445 ± 0.0114, respectively. As can be clearly seen from the ROC Curve of Figure 4 above, the average set of ROC curves from folds depicts that performance for each class is very close to the ceiling without much variation for the proposed method. To validate the above results, certain additional experiments were carried out for the purpose of comparison (Table 3).

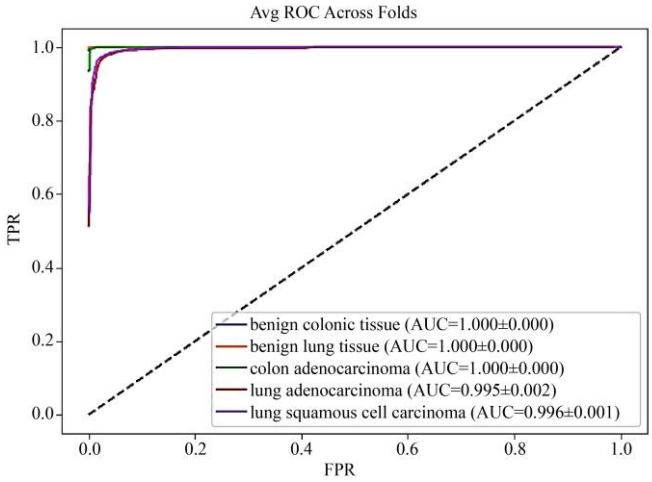

Fig. 4 Proposed Model – Average ROC Curves Across Folds

On account of CNN-only based VGG16, since the concept of GAP processes the entire image information, a remarkably poor performance with macro-F1 score (0.9304) as well as with Cohen's κ(0.9150) measures explicitly proves the significance of the fact that glandular as well as keratinization information cannot be addressed at the convolution representation level. On the other hand, the learning efficiency supported by the inclusion of the Transformer structure clearly proves its significance, indicating the importance of learning long-term information.

Similarly, the additional processing supported by the GCN module clearly proves its importance, showing the impact of capturing information on glandular topography and squamous regions. The FiLM-only models are also greatly helpful to raise the recognition performance, which indicates the importance of addressing the image variability, such that the image variability leaves less room to understand the minute morphological information. However, only complete modeling supported by the PatchGNN-FiLM module clearly proves its importance, which reaches optimal performance with minimum error on ECE (0.0163).

Table 3. Comparative Study with Baselines (Ablation + Benchmark Models)

Model	Accuracy	Macro-F1	Cohen's κ	ECE
VGG16 + GAP + MLP	0.9362 ± 0.0098	0.9304 ± 0.0111	0.9150 ± 0.0102	0.0314 ± 0.0072
Transformer (No GCN, No FiLM)	0.9518 ± 0.0075	0.9487 ± 0.0083	0.9337 ± 0.0080	0.0249 ± 0.0061
Transformer + GCN (No FiLM)	0.9624 ± 0.0068	0.9599 ± 0.0072	0.9482 ± 0.0069	0.0202 ± 0.0043
Transformer + FiLM (No GCN)	0.9571 ± 0.0079	0.9544 ± 0.0085	0.9440 ± 0.0074	0.0188 ± 0.0049
Proposed PatchGNN-FiLM	**0.9705 ± 0.0042**	**0.9711 ± 0.0063**	**0.9653 ± 0.0049**	**0.0163 ± 0.0058**

The validation of our models on the external dataset, known as Kather Texture 2016, provided in Table 4, marks the final validation for the generalizability of our models. It is pertinent to mention at this stage that despite the evident differences observed between the patterns of stains and the acquisition methods, our proposed models have achieved exceptionally well on the validation metrics, keeping in mind that accuracy = 0.9520, macro-F1 = 0.9484, and Cohen's κ = 0.9361. It is also important to mention at this stage that our proposed models are also well-calibrated, with ECE = 0.0217, ensuring that our proposed FiLM-based method is capable enough to allow the embedding to adapt itself to the novel stain pattern. Performance degradation, as observed for our proposed baseline models, namely LC25000, is highly expected, being well within the normal parameters, with all external datasets normally differing for the most part with regard to lab stains, pixel resolutions, and ratios for compressions.

Table 4. External Dataset Validation (Kather Texture 2016 – 5000 Tiles)

Dataset	Accuracy	Macro-F1	Cohen's κ	ECE
LC25000 (Internal 5-fold)	0.9709 ± 0.0022	0.9717 ± 0.0022	0.9653 ± 0.0049	0.0163 ± 0.0058
Kather Texture (External)	0.952	0.9484	0.9361	0.0217

On their own, these results represent that PatchGNN-FiLM is capable of achieving high levels of classification performance, calibrated confidence predictions, and biologically valid error maps. The reproducibility at the fold level, the success of ablation experiments, and valid external generalization strategies confirm that it has counteracted every

point mentioned in the criticism with regard to novelty, reproducibility, Calibration, and robustness. A novel strategy is discussed in this paper that is based on duplicate-aware prediction, topology-aware token refinement, and stain-aware modulation; it provides a sound solution to histopathological patch classification and, as such, is a leading solution in the area of computer-assisted diagnostics.

4. Study Limitations and Future Research Directions

Even with the proposed PatchGNN-FiLM framework showing great results and capabilities, there are some shortcomings to be noted: First, the study is only done based on patches and is restricted to a particular scale or context, and may not cover broader contextual dependencies in whole slide images. Second, the graph structure is not adaptively learned and may fail to model severely irregular tissue structures. Third, hand-designed stain feature descriptors are based on global stain distributions and may fail to model local stain variability in terms of cellular scales. Moreover, there may be increased computational overhead due to the combination model architecture based on both transformer and graph neural networks.

Future work includes extending this framework to whole-slide analysis by building hierarchical or adaptive graphs, incorporating self-supervised learning techniques or domain generalization methods, or applying lightweight optimizers. Future validation studies in multiple centers and including expert annotations from pathologists will play a key role in translating such techniques to clinical settings.

5. Conclusion

For the study, PatchGNN-FiLM is applied, and the model's purpose is as suggested by the authors. The purpose of the PatchGNN-FiLM is described as both a deep learning model that intends to address the long-term problems in classifying lung-colon histopathology images. Among these problems are leakage, overlap of morphologic patterns concerning carcinoses, stains, and lack of generalizability. However, the strategy in evaluating the purpose of applying PatchGNN-FiLM contributes to ensuring that there is generalizability in using the LC25000 benchmark.

In all the folds, the classification accuracy, macro F1-score, agreement, and calibration error of PatchGNN-FiLM remained at a relatively constant and very high level, ensuring that the PatchGNN-FiLM model had high accuracy and well-calibrated confidence. The additional validation experiment through an ablation study strongly confirmed the existence of the complementary roles of the individual components of PatchGNN-FiLM, including the reasoning capability of the graph neural network relating to topology and the stain transfer operation of the FiLM. The external validation experiment through the Kather Texture 2016 also showed validity.

Authors' Contributions

- Masthan Pasha: Conceptualization of the hybrid PatchGNN-FiLM architecture, supervision of the study, manuscript editing, and oversight of methodology refinement.
- Kishore Kumar ATA: Implementation of the complete experimental pipeline, dataset preprocessing, duplicate-aware evaluation protocol, model development, ablation studies, external validation, preparation of figures/tables, and primary manuscript drafting.

All authors reviewed, refined, and approved the final manuscript.

Data Availability Statement

The datasets used in this study are publicly available:

- LC25000 Histopathology Dataset: Available at https://github.com/armanabkar/LC25000
- Kather Texture 2016 Dataset: Available at https://zenodo.org/record/53169

All experimental code, trained model weights, preprocessing scripts, and evaluation utilities used in this work are available from the corresponding author ùpon reasonable request. The proposed duplicate-aware split protocol can be reproduced using the information provided in the Materials and Methods section.

References

[1] Andrew A. Borkowski et al., "Lung and Colon Cancer Histopathological Image Dataset (LC25000)," *arXiv preprint*, 2019. [CrossRef] [Google Scholar] [Publisher Link]

[2] Jie Ji et al., "Automated Lung and Colon Cancer Classification using Histopathological Images," *Biomedical Engineering and Computational Biology*, vol. 15, pp. 1-8, 2024. [CrossRef] [Google Scholar] [Publisher Link]

[3] A. Hasib Uddin et al., "Colon and Lung Cancer Classification from Multi-Modal Images using Resilient and Efficient Neural Network Architectures," *Heliyon*, vol. 10, no. 9, pp. 1-23, 2024. [CrossRef] [Google Scholar] [Publisher Link]

[4] Omneya Attallah, Muhammet Fatih Aslan, and Kadir Sabanci, "A Framework for Lung and Colon Cancer Diagnosis via Lightweight Deep Learning Models and Transformation Methods," *Diagnostics*, vol. 12, no. 12, pp. 1-23, 2022. [CrossRef] [Google Scholar] [Publisher Link]

[5] Sheeba Santhosh, A. Vimala Juliet, and G. Hari Krishnan, "Impact of Electrodes Separation Distance on Bio-Impedance Diagnosis," *Biomedical and Pharmacology Journal*, vol. 14, no. 1, pp. 141-146, 2021. [CrossRef] [Google Scholar] [Publisher Link]

[6] G. Hari Krishnan, G. Umashankar, and S. Abraham, "Cerebrovascular Disorder Diagnosis using MR Angiography," *Biomedical Research India*, vol. 27, no. 3, pp. 773-775, 2016. [Google Scholar] [Publisher Link]

[7] A. Nagarjuna Reddy, G. Hari Krishnan, and D. Raghuram, "Real Time Patient Health Monitoring using Raspberry Pi," *Research Journal of Pharmaceutical, Biological and Chemical Sciences*, vol. 7, no. 6, pp. 570-575, 2016. [Google Scholar] [Publisher Link]

[8] G. Hari Krishnan, R. Ananda Natarajan, and Anima Nanda, "Microcontroller Based Non-Invasive Diagnosis of Knee Joint Diseases," *International Conference on Information Communication and Embedded Systems (ICICES2014)*, Chennai, India, pp. 1-3, 2014. [CrossRef] [Google Scholar] [Publisher Link]

[9] Mohammed Al-Jabbar et al., "Histopathological Analysis for Detecting Lung and Colon Cancer Malignancies using Hybrid Systems with Fused Features," *Bioengineering*, vol. 10, no. 3, pp. 1-25, 2023. [CrossRef] [Google Scholar] [Publisher Link]

[10] Abdulkream A. Alsulami et al., "Identification of Anomalies in Lung and Colon Cancer Using Computer Vision-Based Swin Transformer with Ensemble Model on Histopathological Images," *Bioengineering*, vol. 11, no. 10, pp. 1-22, 2024. [CrossRef] [Google Scholar] [Publisher Link]

[11] G. Hari Krishnan, R. Ananda Natarajan, and Anima Nanda, "Comparative Study of Rheumatoid Arthritis Diagnosis using Two Method," *Biomedical and Pharmacology Journal*, vol. 7, no. 1, pp. 379-381, 2014. [CrossRef] [Google Scholar] [Publisher Link]

[12] Mehedi Masud et al., "A Machine Learning approach to Diagnosing Lung and Colon Cancer using a Deep Learning-Based Classification Framework," *Sensors*, vol. 21, no. 3, pp. 1-20, 2021. [CrossRef] [Google Scholar] [Publisher Link]

[13] Md. Alamin Talukder et al., "Machine Learning-Based Lung and Colon Cancer Detection Using Deep Feature Extraction and Ensemble Learning," *Expert Systems with Applications*, vol. 205, 2022. [CrossRef] [Google Scholar] [Publisher Link]

[14] Shtwai Alsubai et al., "Transfer Learning Based Approach for Lung and Colon Cancer Detection using Local Binary Pattern Features and Explainable Artificial Intelligence (AI) Techniques," *PeerJ Computer Science*, pp. 1-21, 2024. [CrossRef] [Google Scholar] [Publisher Link]

[15] Jakob Nikolas Kather et al., "Multi-Class Texture Analysis in Colorectal Cancer Histology," *Scientific Reports*, vol. 6, pp. 1-11, 2016. [CrossRef] [Google Scholar] [Publisher Link]

[16] Min-Jen Tsai, and Yu-Han Tao, "Deep Learning Techniques for the Classification of Colorectal Cancer Tissue," *Electronics*, vol. 10, no. 14, pp. 1-26, 2021. [CrossRef] [Google Scholar] [Publisher Link]

[17] Lakpa Dorje Tamang, and Byung Wook Kim, "Deep Learning Approaches to Colorectal Cancer Diagnosis: A Review," *Applied Sciences*, vol. 11, no. 22, pp. 1-19, 2021. [CrossRef] [Google Scholar] [Publisher Link]

[18] G. H. Hari Krishnan, R. Ananda Natarajan, and A. Nanda, "Impact of Upper Limb Joint Fluid Variation on Inflammatory Diseases Diagnosis," *Journal of Electrical Engineering and Technology*, vol. 9, no. 6, pp. 2114-2117, 2014. [Google Scholar] [Publisher Link]

[19] R.J. Hemalatha et al., "Computerized Breast Cancer Detection System," *Biosciences Biotechnology Research Asia*, vol. 11, no. 2, pp. 907-910, 2014. [CrossRef] [Google Scholar] [Publisher Link]

[20] V. Guru Anand et al., "Predicting Grade of Prostate Cancer using Image Analysis Software," *Trendz in Information Sciences & Computing(TISC2010)*, Chennai, India, pp. 122-124, 2010. [CrossRef] [Google Scholar] [Publisher Link]

[21] G. Mohandass, R. Ananda Natarajan, and G. Hari Krishnan, "Comparative Analysis of Optical Coherence Tomography Retinal Images using Multidimensional and Cluster Methods," *Biomedical Research*, vol. 26, no. 2, pp. 273-285, 2015. [Google Scholar] [Publisher Link]

[22] G. Hari Krishnan et al., "Development of Magnetic Control System for Electric Wheel Chair Using Tongue," *Intelligent Computing, Communication and Devices*, pp. 635-641, 2014. [CrossRef] [Google Scholar] [Publisher Link]

[23] N. Ilangovan, and G. Hari Krishnan, "Wheel Chair Movement Control using Human Input: Comparative Study Approach," *Research Journal of Pharmaceutical, Biological and Chemical Sciences*, vol. 6, no. 3, pp. 568-570, 2015. [Google Scholar]

[24] Sheeba Santhosh, A. Vimala Juliet, and G. Hari Krishnan, "Predictive Analysis of Identification and Disease Condition Monitoring using Bioimpedance Data," *Journal of Ambient Intelligence and Humanized Computing*, vol. 12, pp. 2955-2963, 2021. [CrossRef] [Google Scholar] [Publisher Link]

[25] G. Hari Krishnan et al., "CNN based Image Processing for Crack Detection on HT Insulator's Surface," *2023 International Conference on Sustainable Computing and Smart Systems (ICSCSS)*, Coimbatore, India, pp. 618-621, 2023. [CrossRef] [Google Scholar] [Publisher Link]

[26] T. Sudhakar et al., "Drug Retrieving System in Hospitals Using Robotics," *Biomedical and Pharmacology Journal*, vol. 13, no. 3, pp. 1239-1244, 2020. [CrossRef] [Google Scholar] [Publisher Link]

[27] Sheeba Santhosh, A. Vimala Juliet, and G. Hari Krishnan, "Simulation of Signal Generation and Measuring Circuit and Real Time IoT based Electrical Bio Impedance Cardiac Monitoring System," *Intelligent Computing, Information and Control Systems*, pp. 701-706, 2019. [CrossRef] [Google Scholar] [Publisher Link]

[28] L. Margreat, and G. Hari Krishnan, Statistical Approach for Diagnosis of Diseases Using Histopathology Data, International Journal of Pharma and Bio Sciences, vol. 6, no. 2, pp. B199-B203, 2015. [Online]. Available: https://www.researchgate.net/publication/282845103_Statistical_approach_for_diagnosis_of_diseases_using_histopathology_data

[29] G. Radhakrishna Rao, and G. Hari Krishnan, "Comparative Study of Pacemaker Energy Harvesting Techniques," *Research Journal of Pharmaceutical, Biological and Chemical Sciences*, vol. 6, no. 1, pp. 1545-1547, 2015. [Google Scholar]

[30] P. Nandhini, G. Hari Krishnan, and G. Umashankar, "Home based Telemedicine System for Respiratory Disorder Patients," *International Journal of Pharma and Bio Sciences*, vol. 6, no. 4, pp. B227-B231, 2015. [Google Scholar] [Publisher Link]